PLOS ONE (ISSN: 1932-6203) (eISSN: 1932-6203) 9: (2) p. e89136. 12 p. (2014)

DOI: 10.1371/journal.pone.0089136

Rac1 Participates in Thermally Induced Alterations of the Cytoskeleton, Cell Morphology and Lipid Rafts, and Regulates the Expression of Heat Shock Proteins in B16F10 Melanoma Cells

Burçin Güngör[1], Imre Gombos[1], Tim Crul[1], Ferhan Ayaydin[2], Lajos Mátés[3], Zsolt Török[1] , László Szabó[4], László Vígh[1] and Ibolya Horváth[1*]

[1]Institute of Biochemistry, Laboratory of Molecular Stress Biology and [2]Laboratory of Cellular Imaging; [3]Institute of Genetics, Laboratory of Cancer Genome Research, Temesvári krt. 62 H-6724 Szeged, [4]Institute of Material and Environmental Chemistry, Department of Functional and Structural Materials, Research Center for Natural Sciences, Pusztaszeri ut 59-67, 1025 Budapest, Hungary.

Abstract

Eukaryotic cells exhibit a characteristic response to hyperthermic treatments involving morphological and cytoskeletetal alterations and induction of heat shock protein synthesis. Small GTPases of the Ras superfamily are known to serve as molecular switches which mediate responses to extracellular stimuli. Here we addressed how small GTPase Rac1 integrates signals from heat stress and induces simultaneously various cellular changes in mammalian cells. Evidencing that Rac1 is implicated in the heat shock response, first we showed that both mild (41.5 °C) and severe (43 °C) heat shock induced membrane translocation of Rac1. Upon the inhibition of the activation (NSC23766) or palmitoylation (2-bromopalmitate) of Rac1, the size of its

plasmamembrane bound pool was significantly decreased. Heat shock induced alterations in the cytoskeleton and cell morphology were prevented using the above inhibitors. Earlier we hypothesized that the level and size distribution pattern of Chol-rich rafts are directly coupled to the triggering mechanism of stress sensing and signaling. As a striking finding, when plasma membrane localization of Rac1 was inhibited we obtained reduced raft domain size at 43 °C. The above documented effects of Rac1 inhibitors were accompanied with a strongly decreased expression of *hsp25* and *hsp70* under both mild and severe heat stress conditions.

Keywords: Rac1, heat stress protein, membrane localization, actin cytoskeleton, cell morphology, rafts, heat sensing and signaling

1. Introduction

Whereas most of the cancer cells exhibit increased levels of the heat shock protein (HSP) subset of molecular chaperones (Jego et al. 2013) the exact mechanism of their elevated expression is still unresolved. One suggestion for HSP overload typical in tumor cells is the ‘‘addiction to chaperones’’ hypothesis which predicts, that addiction is caused by the requirement for HSPs to chaperone the increased protein load that accompanies transformation and the inherent instability of many mutant proteins (Dai et al. 2007) Alterations of lipid profiles have been associated to various disease states and it is suggested that changes of specific lipids are key factors of the onset and evolution of cancer (Vigh et al. 2007; Balogh et al. 2010). The main difference between normal and

tumor cell membrane resides in the actual status of the physical state and nanoplatform (raft) organization (Baritaki et al. 2007). Well highlighting this notion changes of ceramid level of cancer cells is a major factor controlling their apoptotic resistance (Morad and Cabot 2013).

The “membrane thermosensor” hypothesis postulates that heat stress can be sensed by subtle changes in the fluidity and microdomain hyperstructures of membranes influencing membrane-localized stress sensing- and signaling and thus, expression of HSPs (Horváth et al. 1998; Vigh et al. 1998; Balogh et al. 2010). Here we used the B16F10 mouse melanoma cell line, widely applied as model system for studying many aspects of cancer biology including heat shock response. Rho family small GTPase Rac1 drives actin polymerization and is an important integrator of signals from integrins and growth factor receptors (Bustelo et al. 2012), and altered signaling is related to cell transformation, tumor invasion, and metastasis (Han et al. 2001; Aranda et al. 2011). Data suggest that actin filament reorganization is also involved in the process of apoptosis initiated by mild hyperthermia. Destabilization of actin cytoskeletons proceeds with increasing stress temperatures and leads to active reorganization of plasma membrane coincidental to heat-induced shrinkage and rounding of cell shape (Dressler et al. 2005). Based on our former reasoning (Vigh et al. 2005; Gombos et al. 2011) we assumed, that Rac1 controls also the HSP expression in B16 cells by acting as one of the key mediators of stress induced remodeling of surface membrane rafts.

In our present study, the role of Rac1 in the HSP modulator actions of mild heat together with drugs used in 'membrane lipid therapy' have been tested. Established Rac1 specific inhibitors, NSC23766 along with 2-Bromopalmitate – which blocks Rac1 palmitoylation

necessary for interaction with the liquid ordered membrane domains (Navarro-Lérida et al. 2012; Tsai and Philips 2012) have been investigated. Both Rac1 inhibitors tested caused a strongly reduced heat shock protein response (HSR). Apparently this altered HSR was not correlated with visible change in the level of HSF1 phosphorylation. We firstly document, that the functionality of Rac1, and especially palmitoylation, remarkably affects its thermally induced relocalization to the surface membrane. In addition, elevated association of Rac1 to the surface membranes can causally be linked to the earlier reported heat and membrane hyperfluidization induced remodeling of cholesterol enriched membrane microdomains (Nagy et al. 2007; Gombos et al. 2011; Csoboz et al. 2013).

2. Materials and Methods

Cell culture

B16F10 mouse melanoma cells were cultured in RPMI 1640 medium supplemented with 10% FCS and 4 mM L-glutamine. Mouse embryonic fibroblasts (MEFs) were grown in DMEM containing 10% FCS and 4mM L-glutamine. Cells were maintained at 37 °C in a humidified 5% CO_2-atmosphere.

Treatments and reagents

For heat shock treatment, the plates were immersed in a water bath set to the indicated temperature for 1 h. In order to check the localization of Rac1 and F-actin proteins, HSF1 western blotting, mRNA levels of *hsp25* and *hsp70* genes, alterations of cholesterol and

sphingomyelin containing membrane micro-domains, samples were prepared right after heat shock treatments. Rac1 specific inhibitor NSC23766 (NSC) (Santa Cruz Biotechnology) (100μM) and palmitoylation inhibiting compound 2-Bromopalmitate (2-Brp) (Sigma Aldrich) (25μM) was applied for 2 h and 30 min, before heat treatment. These compounds were not present in the medium during heat stress. HSP co-inducer BGP15 (10μM) was added right before heat-shock. Levels of HSP25 and HSP70 proteins were investigated by Western blotting after an overnight recovery of treated cells, after replacement of fresh medium.

Isolation of crude membrane fraction for testing heat induced membrane partitioning of Rac1

B16F10 cells were grown on 10 cm plates and $2x10^7$ cells were used for each sample preparation. Cells heat shocked for 1 h at indicated temperatures were washed twice with ice cold PBS, harvested by scraping on ice and re-suspended in 1 ml of ice cold SCA Buffer (20mM HEPES-KOH pH 7.5, 10mM KCl, 1.5mM $MgCl_2$, 1mM EDTA, 1mM EGTA, 250 mM sucrose and protease inhibitor cocktail (Sigma)). Samples were prepared as described by (DerMardirossian et al. 2006). Pellets were mixed with 1:3 volumes of 3X Laemmli Buffer (Laemmli 1970) and equal amounts of protein samples were subjected to western blot analysis. Membrane was probed with monoclonal Rac1 antibody (clone 23A8, Millipore) (1:1000) then reprobed with Caveolin-1 antibody (C3237, Sigma Aldrich) (1:1000). Expression levels were visualized with Enhanced Chemiluminescence. Band intensities were measured with Alpha View Software v.1.3.0.7..

Testing the plasmamembrane/perimembrane Rac1 localization by confocal microscopy

Following various pretreatments, the B16F10 cells were fixed with 4% paraformaldehyde (PFA), then permeabilized with 0.1% TritonX100. Rac1 antibody (1:100) was used for labeling for 1 h at room temperature which was followed by anti-mouse Alexa488 (A21202, Life Technologies) (1:300) labeling for 1 h at 37 °C. After washings, images were taken with Leica SP5 AOBS confocal laser scanning microscope (Leica) using the 488 argon laser line for excitation and 500-530 spectral filter for emission detection. Images were analyzed by ImageJ software: whole cells and plasma membranes (PM) were drawn around on at least 15 cells/3 views for each treatment. The average intensity of pixels representing the plasma membrane was divided by the average intensity of whole cell in an equatorial focal plane. T-test was calculated. Experiment was repeated 3 times, the results showe the same tendency. Linear region of interest was chosen at every representetive image. Fluorescent intensity of pixels within this region were plotted.

Membrane microdomain size distribution analysis

B16F10 cells were grown in glass-bottom dishes pretreated with inhibitors; NSC 2h and 2-Brp 30 min then heat shocked at 41.5 ^{o}C or 43 ^{o}C, 1h or kept at 37 ^{o}C. Right after, samples were washed and incubated with 1 μM of BODIPY FL C12-sphingomyelin (Avanti) for 10 min at room temperature for labeling the cholesterol enriched raft domains. After washing the cells with RPMI without phenol-red, images were taken by fluorescent microscope applying objective-based total internal reflection (TIR) configuration using 488 nm light for excitation. Iimages were analyzed in CellProfiler

(www.CellProfiler.org) and ImageJ software (http://rsbweb.nih.gov/ij/). The size (theoretical diameter) of each single detected micro-domain was calculated as 2X * (Npix/π)-2, where X is the size of a pixel in nm and Npix is the number of pixels covering the actual domain. The domains we found were sorted into classes according to theoretical diameter. Calculation was done on at least 35 cells for each sample and t test was subjected. Experiment was repeated 3 times,

Monitoring the total cellular F-actin changes induced by heat treatments in B16F10 cells by flow cytometry

Following heat pretreatments (37.0, 41.5 and 43.0 ^{o}C, 1 h) B16F10 cells were trypsinized, washed, collected and then fixed with 4% PFA, permeabilized with 0.1% TritonX100 and labeled by Alexa Flour 647 Phalloidin (200 nM) (A22287, Life Technologies). Measurements were performed with BD Accuri C 6 flow cytometer (BD Biosciences) with 648 laser line for excitation and FL4 channel for detection. Gating was done based on FSC/SSC and FL4A signals. Quantification of the datas were made by using the CFLow Plus 1.0.227.2. software. 3 independent experiments were performed.

Quantification of surface changes of B16F10 cells under various heat stress conditions and in the presence of Rac1 inhibitors, by scanning electron microscopy (SEM)

B16F10 cells were grown on sterile 5 mm cover slips in 24 well plates. After treatments, cells on cover slips wre washed with PBS and fixed with 2.5% glutaraldehyde solution containing 4.5% glucose buffered with 75 mM cacodylate buffer (pH7.2) for 3 h at room temperature. After 3 washes with 100 mM cacodylate buffer, secondary fixation was

done by addition of 1% osmium tetroxide buffered with 50 mM cacodylate (pH 7.2) for 3 h at room temperature. Subsequently, cells were washed with distilled water, dehydrated in an ethanol series (25%, 50%, 75%, 90%,100%) then 1:1 mixture of ethanol/acetone and then kept in pure acetone. Finally critical point drying was performed with CO_2 in E 3000 critical point drying apparatus (Quorum Technologies, Newhaven).The specimens were mounted on adhesive carbon discs, sputter coated with gold in SC7620 Sputter Coater (Quorum Technologies, Newhaven) and images were taken with scanning electron microscope EVO40 (Carl Zeiss GmbH, Oberkochen) at 20.0 kV. Quantification of the image surfaces was done by using ImageJ. Cell borders were drawn and pixel numbers within the borders were obtained and converted to μm^2 unit. For each samples more than 30 cells were calculated and then t-test was calculated.

Confocal laser scanning microscopy for actin imaging in MEF cells treated at various heat stress conditions with Rac1 inhibitors, NSC and 2-Brp

Confocal laser scanning microscopy was performed using Leica SP5 AOBS confocal laser scanning microscope (Leica, Germany) on DMI6000 microscope base. Microscope configuration was the following: objective lenses: HC PL APO 20x (NA:0.7); HCX PL APO lambda blue 63x OIL (N.A: 1.40) ; sampling speed: 200-400Hz; line averaging: 1-2x; pinhole: 1 airy unit; scanning mode: sequential unidirectional; excitation: 405nm laser (DAPI), 633nm HeNe laser (Alexa 647-phalloidin); spectral emission detectors: 417-525 nm (DAPI), 643-746nm (Alexa 647-phalloidin). DAPI and Alexa 647-phalloidin images were pseudocolored blue and red, respectively. Composite images were prepared using ImageJ software (National Institutes of Health, USA, version 1.46r).

qRT-PCR of hsp25 and hsp70 mRNA of B16F10 cells treated at various heat stress conditions with Rac1 inhibitors, NSC and 2-Brp

Right after heat shock or compound administration as outlines in treatment part cells were harvested in lysis buffer for RNA isolation which was performed by using NucleoSpin RNA II kit (Macherey-Nagel). 1 µg of RNA was reverse-transcribed through use of the RevertAid H Minus First Strand cDNA Synthesis Kit (Fermentas). *hsp70 (Mm01159846_s1)*, *hsp25 (Mm00834384_g1)* and *gapdh (Mm99999915_g1)* primers with TaqMan probes (Applied Biosystems) and TaqMan Universal PCR Master Mix (Applied Biosystems) was used to prepare the reaction mixtures according to manufacturers instructions. The PCR runs were performed in BioRad-CFX96 instrument. Relative quantities of mRNAs were normalized to *gapdh*. Data are the mean of three independent experiments.

Western Blotting

In order to check the Rac1 localization and the phosphorylation level of of HSF1 samples were directly harvested in Laemmli Buffer after the treatments. In the case of checking protein expression levels of HSP25 and HSP70, after overnight recovery at 37 °C, cell lysates were prepared in Laemmli Buffer. Equal amounts of proteins were loaded to 15% or 10% SDS gels according to size of the protein of interest and western blotting was performed. Membranes were probed with monoclonal (mAb) Rac1, Caveolin-1, HSP25 (SPA 801, Stressgen), HSP70 (SPA 810, Stressgen), monoclonal HSF1 (Clones

4B4+10H4+10H8, Thermo Scientific), and Gapdh (Sigma-Aldrich) antibodies as indicated on the figures. Expression levels were visualized with Enhanced Chemiluminescence (Amersham, USA). Band intensities were measured with Alpha View Software v.1.3.0.7. (Alpha Innotech, USA). Data are the mean of three independent experiments.

3. Results

3/1 Heat stress triggers the translocation of Rac1 protein to membranes in B16F10 cells

Earlier it was suggested, that the small GTP-binding protein Rac1 may play a critical role in the early phase of heat stress management (Han et al. 2001; Vigh et al. 2005) Since translocation of Rac1 to the plasma membrane is assumed as an essential step for activating downstream effectors (del Pozo et al. 2004) and for remodelling membrane microdomains (Navarro-Lérida et al. 2012) first the effect of heat stress on membrane fraction localization of Rac1 was investigated on the highly metastatic B16F10 melanoma cells. Based on the comparison of the calculated relative band intensities of western blots (37 ^{o}C=100; 41.5 ^{o}C=132; 42 ^{o}C= 310 ; 43.0 ^{o}C= 255) exposing cells to 41.5 ^{o}C did not significantly influence Rac1 membrane association. By contrary, thermal treatments at 42 and 43 ^{o}C, respectively caused a highly elevated association of Rac1 with cell membranes (**Fig.1a**). Since Rac1 is also localized to endomembranes, like mitochondria (Velaithan et al. 2011) where it is a binding partner of Bcl-2 and stabilizes its anti-apoptotic activity, to demonstrate the heat stress induced alterations of plasma membrane/perimembrane (PM) localization of Rac1 we used confocal microscopy.

Following thermal treatments (41.5 ^{o}C; 43.0 ^{o}C) cells were fixed, permeabilized and Rac1 immunostaning was performed. The confocal microscopy results indicate, that upon elevation of temperature to a clinically relevant range (41.5 ^{o}C) Rac1 is directed to the plasma membrane (**Fig.1b,c**). Further increasing the temperature to 43.0 ^{o}C caused no significant additional elevation in the PM associated Rac1 pool. Inhibition of Rac1 activity by the small molecule NSC, (Gao et al. 2004)which binds specifically into a surface groove known to be critical for its GEF interaction, slightly but significantly ($p<0.05$) reduced PM translocation under mild heat condition (**Fig.1c**). Recent work of Del Pozo and co-workers identified palmitoylation of Rac1 as a key mechanism controlling its membrane partitioning (Navarro-Lérida et al. 2012). Pretreatment of cells with 2-Brp, an effective inhibitor of protein palmitoylation *in vivo* we obtained significant loss of both mild ($p<0.01$) and severe ($p<0.05$) heat induced PM-localization of Rac1 (**Fig.1c**). It is noted, that a small, but significant reduction of Rac1 PM localization was observed even in control cells upon 2-Brp administration confirming the central role of palmitoylation in the subcellular compartmentalization of Rac1.

3/2 Palmitoylation of Rac1 controls the heat induced reorganization of PM microdomains in B16F10 melanoma:TIRF microscopy analysis

To unravel the possible mechanisms underlying the capability of various membrane fluidizers for heat shock gene activation, we earlier documented that, apart from overall membrane hyperfluidization, a distinct reorganization of cholesterol and sphingomyelin rich microdomains (“rafts”) may also be required for the generation and transmission of stress signals to activate *hsp* genes in B16F10 cells (Nagy et al. 2007). Recently we have

also shown, that such a reorganization of lipid rafts must be a key determinant in the pleiotropic effects of hyperthermia leading ultimately to cellular adaptation or lethality (Csoboz et al. 2013). Rac1 palmitoylation state was shown to regulate both the fluidity and the domain organization of the PM (Navarro-Lérida et al. 2012). Taken together, next we tested the consequences of palmitoylation inhibitor on membrane microdomain organization with TIR microscopy using BODIPY FL C12-sphingomyelin label on heat treated B16F10 cells. The domain size was analyzed with the freeware ImageJ software (www.uhnresearch.ca/facilities/wcif/imagej), domains were segmented with its fast Fourier transform (FFT) bandpass filter and the nucleus counter plug-in. The sphingomyelin probe-labelled domains were separated into five classes according to their sizes (**Fig.2b**). The average diameter of domains was clearly increased upon temperature elevations and this tendency was not affected at 41.5 ^{o}C by pretreatment with 2-Brp. However, under severe heat shock condition 2-Brp administration prevented raft remodeling, the forming of larger domain sizes (**Fig. 2a,b**). Interestingly however, 2-Brp treatment resulted in higher average domain size even at growth temperature. This domain size was near to what was observed in 2-Brp treated and 43 °C exposed cells plasma membrane. It is well established, that the reversible palmitoylation critically controls the transient membrane tethering of a large number of peripheral membrane proteins. Little is known about how the palmitoylation machinery governs their defined localization and function (Rocks et al. 2010). The complete elucidation of the effect of 2-Brp on lipid raft disarrangement awaits further studies and it is in progress in our laboratory. Namely, preparation of B16F10 Rac1 palmitoylation incompetent mutant cells is underway by using the combined “Recombinase Mediated Cassette Exchange”

(RMCE) and „Sleeping Beauty" (SB) gene transfer method allowing the expression of the genes under their endogenous promoter (Mátés 2011).

3/3 Monitoring the heat induced changes in cytoskeletal F-actin and cell morphologies by fluorescence imaging and scanning electron microscopy (SEM) in B16F10 cells.

Active stress response of mammalian cells is classified as sequential and discontinuous heat-induced processes (Coakley 1987; de Gannes et al. 1998; Beuthan et al. 2004). While cell morphology, adhesion behavior and integrity of surface membranes were shown to be unaffected at mild heat stress (40-41 ^{o}C) the surface rougness of MX1 breast cancer cells increased as a consequence of the destabilization of actin cytoskeletons (Dressler et al. 2005). Monitoring the heat induced changes in the level of cytoskeletal F-actin following prior heat treatments (37.0, 41.5 and 43.0 ^{o}C, 1 h), B16F10 cells were labeled with Alexa Flour 647 conjugated to phalloidin. As an evidence on the heat induced destabilization of F-actin network, flow cytometry investigation exhibited a gradual and drastic reduction of F-actin levels upon heat treatments (**Fig.3a**).

Early studies with Rho family of GTP binding proteins revealed that they play major roles in regulating remodeling of the actin cytoskeleton, induced by stress and extracellular signals. In fact, rearrangements of actin filaments accompanied by striking changes of cell shapes was reported at comparatively mild heat stress conditions using MX1 breast cancer cells (Dressler et al. 2005). Taken together, to follow changes of morphological features next we applied SEM under conditions where distinct reorganization of surface membrane microdomains have already been documented (see **Fig.2**). Based on the calculations of cell surface areas, neither heat treatment at 41.5 ^{o}C,

nor the administration of Rac1 inhibitors, NSC and 2-Brp caused remarkable changes in cell morphology (**Fig.3b**). Thermotreatment performed at 43.0 ^{o}C, resulted apparently in heat-induced shrinkage and rounding of cells, (**Fig.3b**) which led to a significant reduction in the calculated cell surface areas. When heat stress at 43.0 ^{o}C was performed in the presence of either the NSC or 2-Brp, this effect was completely absent (**Fig.3c**), clearly pointing to the key role of Rac1 in heat induced changes in cell morphology.

3/4 Microscopy imaging of Rac1-mediated reorganization of actin fibers upon heat stress in MEF cells.

As discussed before, heat stress induced changes in cell shape and cytoskeleton are well documented using various microscopy and imaging based methods. Both microtubules and actin filaments are affected by heat stress in a variety of organisms (Wiegant et al. 1987; Holubarova et al. 2000; Malerba et al. 2010) Given the importance of Rac1 in actin cytoskeletal organization, we have used Rac1 specific inhibitor NSC, palmitoylation inhibitor (2-Brp) and confocal laser scanning microscopy to assess the potential role of Rac1 on actin fiber organization during heat stress (**Fig.4**). Flat and well-spread fibroblasts are ideally suited for actin labeling and analysis, hence MEF cells are choosen for microscopy analysis of actin reorganization experiments.

Cells w/wo inhibitor pretreatement were subjected to either mild (41.5 ºC) or severe heat stress (43 ºC). Control cells were also treated similarly but kept at 37 ºC. Fixed cells were stained with fluorescent phalloidin to detect actin filaments (see Methods). Mild heat stress did not cause significant reorganization of actin filaments in control or Rac1 inhibitor-treated cells. Actin rich cell protrusions, and several filopodia and lamellipodia

were detectable. On the other hand severe heat stress treatment at 43 ºC caused considerable fragmentation of fine actin network in control cells. Inhibition of Rac1 with NSC prevented this fragmentation considerably: long and intact actin fibers were still detectable in NSC treated cells (**Fig.4**). Cell migration and spreading is driven by actin polymerization and actin stress fibers (Kovac et al. 2013). Control MEF cells exhibited more rounded trapezoid-like cell morphology at 43 ºC indicating reduced spreading and migratory behavior due to disintegration of actin fibers at this temperature. NSC treated-cells, on the other hand, displayed slender, elongated morphology resembling control cells at 37 ºC (**Fig.4**).

Rac1 is shown to be modified by palmitoylation at the carboxy terminal. This modification targets Rac1 for stabilization at actin cytoskeleton-linked ordered membrane regions at the plasma membrane (Navarro-Lérida et al. 2012) Using a palmitoylation inhibitor 2-Brp we have tested actin morphology of MEF cells following mild and severe heat stress treatment. Similar to control and NSC-treated cells, at 41.5 ºC, cells did not display significant actin depolymerization. Elongated cells with actin-rich protrusions were very often detected in 2-Brp treated cells at 41.5 ºC. At 43 ºC, 2-Brp inhibition of palmitoylation resulted in better preserved, intact actin fibers and elongated actin-rich protrusions. Similar to NSC treated cells, only a moderate actin depolymerization was detectable (**Fig.4**). Together with previous data in this article, these data further confirm the Rac1 palmitoylation-dependent disorganization of actin filaments upon severe heat stress treatment. Although this inhibitor does not inhibit specifically and exlusively the Rac1 palmitoylation, according to Navarro-Lérida et al. (2012), using this short inhibiting time period (30 min) affects mainly Rac1 palmitoylation. Based on the previous report of

Navarro-Lérida et al. (2012) it is tempting to speculate that reduced palmitoylation of Rac1 blocks Rac1 plasma membrane relocalization and consequently downregulates actin fiber disorganization following heat stress treatment.

3/5 Effect of Rac1 inhibition by the administration of 2-Brp and NSC on inducable hsp25 and hsp70 gene levels

In previous studies we have shown the elevated gene expression levels of *hsp25* and *hsp70* under stress conditions in B16F10 cells (Nagy et al. 2007; Balogh et al. 2010; Péter et al. 2012). In order to investigate the possible role of Rac1 in HSR the effect of Rac1 inhibitors NSC and 2-Brp were tested using quantitative RT-PCR. Administration of NSC decreased the mRNA levels of both *hsp25* and *hsp70* levels under mild (41.5 °C) heat shock. What is more the hsp co-inducing activity of BGP15 (Crul et al. 2013) was also inhibited. Under severe heat shock (43 °C) both mRNA levels were drastically inhibited by Rac1 inhibitor NSC. In cells heat treated at 41.5 °C administration of 2-Brp displayed inhibitory effect both on *hsp25* and *hsp70* mRNA induction, though the inhibition was more pronounced for *hsp70*. However, at severe heat stress (43 °C) the palmitoylation inhibitor affected far more the *hsp25* than *hsp70* mRNA inducibility (**Fig.5**).

3/6 Heat shock response monitored at protein level (HSP25 and HSP70)

In order to confirm the changes in heat shock protein response by inhibiting Rac1 activity and membrane association, the levels of HSP25 and HSP70 proteins were measured by Western blotting. B16 F10 cells were exposed to compound administrations and stress

conditions as indicated in **Fig 6a**. The elevated expression of HSP25 and HSP70 proteins induced both by mild and severe heat stress was inhibited by the specific Rac1 inhibitor, NSC. Co-inducing the HSR at 41.5 °C with the hydroximic acid BGP15 was remarkably diminished by the administration of NSC. Importantly, the effect of the inhibition of different Rac1 functions upon HSP synthesis was apparently more pronounced under mild heat shock conditions (**Fig.6b**).

3/7 Effect of Rac1 inhibition by the administration of 2-Brp and NSC on HSF1 phosphorylation level

Expression of the HSPs is mediated through the activation of the heat shock transcription factors, of which HSF1 is the master regulator in vertebrates (Akerfelt et al. 2010). As a central dogma predicts, HSF1, which binds to and activates a conserved regulatory site, the heat shock element located in the promoters of heat-inducible *hsp* genes. Under stress conditions, HSF1 homotrimerizes, localizes to the nucleus, becomes transcriptionally competent and is hyperphosphorylated. Here we showed that indeed, HSF1 hyperphosphorylation was proportional to the severity of the heat shock, however neither NSC, nor 2-Brp modulated the heat induced phosphorylation level of HSF1. Since the levels of the transcription of both *hsp25* and *hsp70* were equally and strongly affected by Rac1 inhibitors we applied, it is feasible that such a Rac1 mediated effect on hs-gene transcription does not involve the change of the net phosphorylation of HSF1 (**Fig.7**). In fact, the DNA-binding and transactivation capacity of HSF1 are coordinately regulated through multiple posttranslational modulations (like acetylation), protein–protein interactions and subcellular localization (Akerfelt et al. 2010). In addition, heat shock

gene expression is thought to be controlled at the level of promoter clearance (Wu and Snyder 2008). Accordingly, the expression of heat shock genes should be particularly sensitive to the cellular level of Pol II elongation factors. A variety of Pol II elongation factors are recruited to sites of heat shock gene expression during heat shock (Gerber et al. 2005). However, the signalling pathways responsible for RNA pol activation remain largely unclear.

4.Discussion

Since a small GTPase Rac1 has been suggested to participate in the cellular response to various kinds of stresses, we examined whether Rac1 is involved in several features of the heat shock response under mild (41.5 °C) and severe (43 °C) heat shock conditions. Earlier it was assumed, that increase in intracellular calcium, well documented also under heat stress conditions in our lab (Balogh et al. 2005), is the major regulator of the activation and membrane translocation of Rac1 (Price et al. 2003). The initiation of Rac1 signaling requires also among othere GTP loading and a posttranslational modification, namely palmitoylation (Navarro-Lérida et al. 2012). Palmitoylation targets Rac1 for stabilization of actin cytoskeleton-linked cholesterol-rich liquid-ordered (Lo) plasma membrane microdomains. Here we showed that both moderate and severe heat shock induces membrane translocation of Rac1 and the translocation could be blocked partially by using selective Rac1 activity inhibitor NSC and palmitoylation inhibitor 2-Brp.

Monitoring the patterns of surface membrane microdomains by confocal- and ultrasensitive single molecular microscopy we established a phenomenological relationship between specific distribution of lipid nanostructures (“rafts”) and the

concomitant changes in the level of HSPs (Nagy et al. 2007; Brameshuber et al. 2010; Balogh et al. 2011; Gombos et al. 2011). Here we shown that decrease of the percentage of larger plasma membrane microdomains (929-1136 nm and 1137< nm) on the expense of their smaller counterparts is paralleled with reduction in HSR. We also document that under conditions when plasma membrane localization of Rac1 is inhibited by 2-Brp administration there is a remarkable decrease in raft domain size. Taken together, our findings further corroborate the hypothesis that the level and size distribution pattern of Chol-rich lipid rafts is very likely participate in the early steps of the mechanism of raft-associated stress sensing and signaling (Vigh et al. 2007). The lipid raft hypothesis postulates that primarily the selective interactions among sphingolipids, cholesterol and membrane proteins contribute to lateral membrane heterogeneity (Escribá et al. 2008). Although experimental data support the cholesterol-dependent nano-scale membrane heterogeneity and selective domain formation solely upon raft cross-linking (Paladino et al. 2007; Zech et al. 2009), the mechanisms that govern such associations in live cell membranes during heat stress remain unclear (Horváth et al. 2012).

It is known that both microtubules and actin filaments are affected by heat stress in a variety of organisms and Rac1 was shown to play important roles in cytoskeletal organization. Indeed, both Rac1 inhibitor NSC and palmitoylation inhibitor 2-Brp prevented the severe heat stress induced changes in cell shape and cytoskeleton as documented using confocal microscopy and SEM imaging based methods. In order to make a more profound investigation to assess the potential role of Rac1 on actin fiber organization during heat stress, next we applied confocal laser scanning microscopy using the flat and well-spread MEF fibroblast model. Thermal treatment performed at

43.0 ^{o}C resulted apparently in heat-induced rearrangements of actin filaments and shrinkage and rounding of cells, which then led to a significant reduction in the calculated cell surface areas. When severe heat stress was performed in the presence of either the NSC or 2-Brp, this effect was completely absent clearly pointing to the central role of Rac1 in heat induced changes in cell morphology.

As a consequence of inhibiting either activity or PM relocalization of Rac1, parallel we observed a clear decrease in *hsp25* mRNA level both under mild and severe heat stress conditions. Noteworthy, whereas administration of both Rac1 inhibitors caused a sizable decrease in the formation of *hsp70* mRNA, at 41.5 °C as well, in contrast to NSC, 2-Brp remained seemingly uneffective at heat stress condition.

The same observations prevailed concerning HSP protein level changes in the case of using NSC. On the other hand, 2-Brp treatment caused no significant change in the HSR of the melanoma cells at protein level (data are not shown).

It is noted, that the finding that the HSP co-inducer BGP15-enhanced activation of HSP expression involves the Rac1 signaling (Gombos et al. 2011) gained full support also in the present study. As noted before, since we fully aware of the unspecific and pleiotropic effect of 2-Brp, further studies are underway in our laboratory with palmitolylation incompetent, constitutively active and dominant negative Rac1 mutant B16F10 cells.

Finally, as we discussed above, seemingly neither NSC nor 2-Brp affected the detectable level of HSF1 phosphorylation. It is noted, however, that in their early studies aimed at investigating the role of Rac1 in the JNK activation and HSF1, Han and co-workers also concluded that although a specific signal pathway involving Rac1 is likely linked to the heat shock-induced HSF activation and HSP expression, a Rac1-independent mechanism

is also involved, especially in the severe heat shock response. Therefore, Rac1 activation may be necessary, but not sufficient, for thermally induced activation of HSF1 (Han et al. 2001).

Although the mode of HSF1 activation follows likely the same principle upon various stresses, there are stimulus-specific differences, arguing against a single common signal pathway to activate HSF1. HSF1 itself could act as a hub for stress-induced gene activation, providing a relay point for downstream signalling of different stress stimuli. As Sistonen and co-workers suggested (Akerfelt et al. 2010), the activation and attenuation mechanisms of HSFs require additional mechanistic insights. The roles of the multiple signal transduction pathways involved in post-translational regulation of HSFs are only now being discovered and are clearly more complex than anticipated.

Figure legends

Fig.1 Rac1 translocation to membranes as a result of Rac1 inhibitor and heat shock treatment (**a)** Rac1 localization to the crude membrane fraction upon heat-shock treatment. B16F10 cells were subjected to heat shock at indicated temperatures for 1 h. Right after crude membrane fraction was isolated and solubilised in Laemmli buffer. Equal amounts of proteins were run for Western blotting. Rac1 probing was performed for the membrane and caveolin immunostaining was used for normalization. Change in normalized Rac1 band intensities are: 37 °C =100, 41.5 °C =132, 42 °C =310, 43 °C =255. (**b)** Visualization of Rac1 association to plasma membrane. B16F10 cells in glass bottom plates were kept in water bath at indicated temperatures for 1 h. Then cells were fixed, permeabilized and immunoreacted with Rac1 mAb then probed with Alexa488

labelled secondary antibody using confocal microscopy. Intensity profiles of region of interests on confocal images (indicated with white lines) are shown. Black arrows point out PM. Red curve represents 43 °C, blue curve 41.5 °C and black curve 37 °C. (**c**)The effect of Rac1 inhibitor administration on Rac1-membrane binding under heat stress conditions. Cells were treated/or not with Rac1 inhibitor NSC and 2-Brp and heat shocked/or not, then immunostained as above. Confocal images were taken and 15 cells/3 views for each treatment were quantified by ImageJ. The bars represent the fluorescence intensity of plasma membrane versus the fluorescence intensity of the whole cell. Black bars represent no inhibitor treated, white bars the NSC and gray bars the 2-Brp treated cells. ± SEM are shown, n =3 and student's t-test was subjected for statistical analysis. * : $p<0.05$; ** : $p<0.01$; *** : $p<0.001$

Fig.2 Change in the size of plasma membrane microdomains as a function of temperature and 2-Brp treatment. **(a)** 2-Brp was added/or not to samples for 30 min and then they were heat treated at 41.5 °C or 43 °C or kept at 37 °C for 1 h. After fPEG-cholesterol labelling and TIR microscopy, the domain distribution was analyzed with ImageJ and CellProfiler softwares and the average domain sizes are shown. (**b**) From the experiment shown on (**a**) the plasma membrane microdomains were separated into five classes according to their sizes. The data shown are mean values ± SEM, n = 3.

Fig.3 F-actin and cell morphology changes in B16F10 cells under heat shock conditions **(a)** Measurement of heat stress triggered F-actin alterations by using Flow cytometry. After heat stress, cells were collected by trypsinization, fixed and labelled with Alexa 647 phalloidin. Flow cytometry measurement was done by BD Accuri C 6 cytometer and

CFLow Plus 1.0.227.2. software was used for data analysis. (**b)** Surface area changes of B16F10 cells as an effect of heat shock and Rac1 inhibitor administration. B16F10 cells were subjected to stress conditions at 41.5 °C and 43 °C or kept at 37 °C with or without inhibitor administration as indicated and samples were fixed for SEM imaging. From the SEM images, 30 cells were chosen to calculate surface area by ImageJ software. Black bars show no inhibitor treatment, white and gray bars respresent NSC and 2-Brp administrations, respectively. 3 independent experiments' data was shown along with its standart deviation. Student's t-test was used for statistical analysis * : $p<0.05$; ** : $p<0.01$; *** : $p<0.001$.(**c)** Representative SEM photos of 37 °C and 43 °C untreated, and 43 °C NSC or 2-Brp treated cells.

Fig.4 The effect of Rac1 inhibitors on the actin filaments of heat and Rac1 inhibitor - treated MEF cells. Cells were subjected to temperature treatmets w/wo NSC or 2-Brp treatment. After fixation and permeabilization cells were labelled with Alexa 647-phalloidin (red, actin) and DAPI (blue, nuclei) and confocal miroscopy was used for immunlocalization. Scalebar 40μm.

Fig.5 Effect of Rac1 inhibitors 2-Brp and NSC on *hsp25* and *hsp70* gene expression levels under heat shock conditions.. B16F10 cells were either treated/or not with 2-Brp or NSC for 30 min or 2 h respectively, then exposed/or not to indicated heat shock temperatures for 1 h. Total RNA was isolated right after heat shock and the expression levels of *hsp70* and *hsp25* mRNAs were measured by quantitative RT-PCR and were normalized to *Gapdh*. If BGP15 (HSP co-inducer) was used it was administered at 10 μM

concentration during heat shock. Data shown are fold changes compared to the mRNA levels measured in 37 °C samples. n = 3, data show ± SEM.

Fig.6 Effect of Rac1 inhibitor 2-Brp and NSC on HSP25 and HSP70 protein expression levels under heat shock conditions. Cells were treated as for **Fig.5** and were collected after an overnight recovery at 37 °C. (**a)** Western blotting was performed for equal amounts of total protein samples. Membrane was probed with anti-HSP25 and anti-HSP70 antibodies and anti-Gapdh was used for the normalization. (**b**) Quantification of the band intensities of protein expression levels were made by Alpha View Software v.1.3.0.7. and normalized to Gapdh. When calculated the fold changes, protein levels of 41.5 °C samples were considered as 100. n = 3 data show ± SD.

Fig.7 Effect of Rac1 inhibition on hyperphosphorylation level of HSF1. B16F10 cells were treated or not with inhibitors (NSC or 2-Brp) prior to the indicated heat shock conditions. Right after, samples were harvested and equal amounts were used for western blotting. Membrane was probed with anti-HSF1 and anti-Gapdh antibody.

Acknowledgement

This study was supported by grants from the Hungarian Basic Research Fund (OTKA, NK100857, K82097), by the Hungarian National Development Agency (TAMOP-4.2.2/B-10/1-2010-0012). The authors would like to thank Árpád Párducz for his advices in SEM picture analysis.

References

Akerfelt M, Morimoto RI, Sistonen L (2010) Heat shock factors: integrators of cell stress, development and lifespan. Nat Rev Mol Cell Biol 11:545–555.

Aranda JF, Reglero-Real N, Kremer L, et al. (2011) MYADM regulates Rac1 targeting to ordered membranes required for cell spreading and migration. Mol Biol Cell 22:1252–62. doi: 10.1091/mbc.E10-11-0910

Balogh G, Horváth I, Nagy E, et al. (2005) The hyperfluidization of mammalian cell membranes acts as a signal to initiate the heat shock protein response. FEBS J 272:6077–6086.

Balogh G, Maulucci G, Gombos I, et al. (2011) Heat stress causes spatially-distinct membrane re-modelling in K562 leukemia cells. PLoS One 6:e21182. doi: 10.1371/journal.pone.0021182

Balogh G, Péter M, Liebisch G, et al. (2010) Lipidomics reveals membrane lipid remodelling and release of potential lipid mediators during early stress responses in a murine melanoma cell line. Biochim Biophys Acta 1801:1036–1047.

Baritaki S, Apostolakis S, Kanellou P, et al. (2007) Reversal of tumor resistance to apoptotic stimuli by alteration of membrane fluidity: therapeutic implications. Adv Cancer Res 98:149–190.

Beuthan J, Dressler C, Minet O (2004) Laser induced fluorescence detection of quantum dots redistributed in thermally stressed tumor cells. Laser Phys 14:213–219.

Brameshuber M, Weghuber J, Ruprecht V, et al. (2010) Imaging of mobile long-lived nanoplatforms in the live cell plasma membrane. J Biol Chem 285:41765–41771.

Bustelo XR, Ojeda V, Barreira M, et al. (2012) Rac-ing to the plasma membrane: the long and complex work commute of Rac1 during cell signaling. Small GTPases 3:60–6. doi: 10.4161/sgtp.19111

Coakley WT (1987) Hyperthermia effects on the cytoskeleton and on cell morphology. Symp Soc Exp Biol 41:187–211.

Crul T, Toth N, Piotto S, et al. (2013) Hydroximic Acid Derivatives : Pleiotrophic Hsp Co-Inducers Restoring Homeostasis and Robustness. Curr. Pharm. Des. 19:

Csoboz B, Balogh GE, Kusz E, et al. (2013) Membrane fluidity matters: hyperthermia from the aspects of lipids and membranes. Int J Hyperthermia 29:491–9. doi: 10.3109/02656736.2013.808765

Dai C, Whitesell L, Rogers AB, Lindquist S (2007) Heat shock factor 1 is a powerful multifaceted modifier of carcinogenesis. Cell 130:1005–18. doi: 10.1016/j.cell.2007.07.020

DerMardirossian C, Rocklin G, Seo J-Y, Bokoch GM (2006) Phosphorylation of RhoGDI by Src regulates Rho GTPase binding and cytosol-membrane cycling. Mol Biol Cell 17:4760–8. doi: 10.1091/mbc.E06-06-0533

Dressler C, Minet O, Beuthan J, et al. (2005) Microscopical heat stress investigations under application of quantum dots. J Biomed Opt 10:41209. doi: 10.1117/1.2001674

Escribá P V, González-Ros JM, Goñi FM, et al. (2008) Membranes: a meeting point for lipids, proteins and therapies. J Cell Mol Med 12:829–875.

De Gannes FM, Merle M, Canioni P, Voisin PJ (1998) Metabolic and cellular characterization of immortalized human microglial cells under heat stress. Neurochem Int 33:61–73.

Gao Y, Dickerson JB, Guo F, et al. (2004) Rational design and characterization of a Rac GTPase-specific small molecule inhibitor. Proc Natl Acad Sci U S A 101:7618–23. doi: 10.1073/pnas.0307512101

Gerber M, Tenney K, Conaway JW, et al. (2005) Regulation of heat shock gene expression by RNA polymerase II elongation factor, Elongin A. J Biol Chem 280:4017–20. doi: 10.1074/jbc.C400487200

Gombos I, Crul T, Piotto S, et al. (2011) Membrane-lipid therapy in operation: The HSP co-inducer BGP-15 activates stress signal transduction pathways by remodeling plasma membrane rafts. PLoS One accepted:e28818.

Han SI, Oh SY, Woo SH, et al. (2001) Implication of a small GTPase Rac1 in the activation of c-Jun N-terminal kinase and heat shock factor in response to heat shock. J Biol Chem 276:1889–1895.

Holubarova A, Müller P, Svoboda A (2000) A response of yeast cells to heat stress: Cell viability and the stability of cytoskeletal structures. Scr MEDICA 73:381–392.

Horváth I, Glatz A, Nakamoto H, et al. (2012) Heat shock response in photosynthetic organisms: membrane and lipid connections. Prog Lipid Res 51:208–220.

Horváth I, Glatz A, Varvasovszki V, et al. (1998) Membrane physical state controls the signaling mechanism of the heat shock response in Synechocystis PCC 6803: identification of hsp17 as a “fluidity gene”. Proc Natl Acad Sci U S A 95:3513–3518.

Jego G, Hazoumé A, Seigneuric R, Garrido C (2013) Targeting heat shock proteins in cancer. Cancer Lett 332:275–85. doi: 10.1016/j.canlet.2010.10.014

Kovac B, Teo JL, Mäkelä TP, Vallenius T (2013) Assembly of non-contractile dorsal stress fibers requires α-actinin-1 and Rac1 in migrating and spreading cells. J Cell Sci 126:263–73. doi: 10.1242/jcs.115063

Laemmli UK (1970) Cleavage of structural proteins during the assembly of the head of bacteriophage T4. Nature 227:680–5.

Malerba M, Crosti P, Cerana R (2010) Effect of heat stress on actin cytoskeleton and endoplasmic reticulum of tobacco BY-2 cultured cells and its inhibition by Co2+. Protoplasma 239:23–30. doi: 10.1007/s00709-009-0078-z

Mátés L (2011) Rodent transgenesis mediated by a novel hyperactive Sleeping Beauty transposon system. Methods Mol Biol 738:87–99. doi: 10.1007/978-1-61779-099-7_6

Morad SAF, Cabot MC (2013) Ceramide-orchestrated signalling in cancer cells. Nat Rev Cancer 13:51–65. doi: 10.1038/nrc3398

Nagy E, Balogi Z, Gombos I, et al. (2007) Hyperfluidization-coupled membrane microdomain reorganization is linked to activation of the heat shock response in a murine melanoma cell line. Proc Natl Acad Sci U S A 104:7945–7950.

Navarro-Lérida I, Sánchez-Perales S, Calvo M, et al. (2012) A palmitoylation switch mechanism regulates Rac1 function and membrane organization. EMBO J 31:534–51. doi: 10.1038/emboj.2011.446

Paladino S, Sarnataro D, Tivodar S, Zurzolo C (2007) Oligomerization is a specific requirement for apical sorting of glycosyl-phosphatidylinositol-anchored proteins but not for non-raft-associated apical proteins. Traffic 8:251–8. doi: 10.1111/j.1600-0854.2006.00522.x

Péter M, Balogh G, Gombos I, et al. (2012) Nutritional lipid supply can control the heat shock response of B16 melanoma cells in culture. Mol Membr Biol 29:274–289.

Del Pozo MA, Alderson NB, Kiosses WB, et al. (2004) Integrins regulate Rac targeting by internalization of membrane domains. Science (80-) 303:839–842.

Price LS, Langeslag M, ten Klooster JP, et al. (2003) Calcium signaling regulates translocation and activation of Rac. J Biol Chem 278:39413–21. doi: 10.1074/jbc.M302083200

Rocks O, Gerauer M, Vartak N, et al. (2010) The palmitoylation machinery is a spatially organizing system for peripheral membrane proteins. Cell 141:458–71. doi: 10.1016/j.cell.2010.04.007

Tsai FD, Philips MR (2012) Rac1 gets fattier. EMBO J 31:517–8. doi: 10.1038/emboj.2011.481

Velaithan R, Kang J, Hirpara JL, et al. (2011) The small GTPase Rac1 is a novel binding partner of Bcl-2 and stabilizes its antiapoptotic activity. Blood 117:6214–26. doi: 10.1182/blood-2010-08-301283

Vigh L, Escribá P V, Sonnleitner A, et al. (2005) The significance of lipid composition for membrane activity: new concepts and ways of assessing function. Prog Lipid Res 44:303–344.

Vigh L, Horváth I, Maresca B, Harwood JL (2007) Can the stress protein response be controlled by "membrane-lipid therapy"? Trends Biochem Sci 32:357–363.

Vigh L, Maresca B, Harwood JL (1998) Does the membrane's physical state control the expression of heat shock and other genes? Trends Biochem Sci 23:369–374.

Wiegant FA, van Bergen en Henegouwen PM, van Dongen G, Linnemans WA (1987) Stress-induced thermotolerance of the cytoskeleton of mouse neuroblastoma N2A cells and rat Reuber H35 hepatoma cells. Cancer Res 47:1674–80.

Wu JQ, Snyder M (2008) RNA polymerase II stalling: loading at the start prepares genes for a sprint. Genome Biol 9:220. doi: 10.1186/gb-2008-9-5-220

Zech T, Ejsing CS, Gaus K, et al. (2009) Accumulation of raft lipids in T-cell plasma membrane domains engaged in TCR signalling. EMBO J 28:466–476.

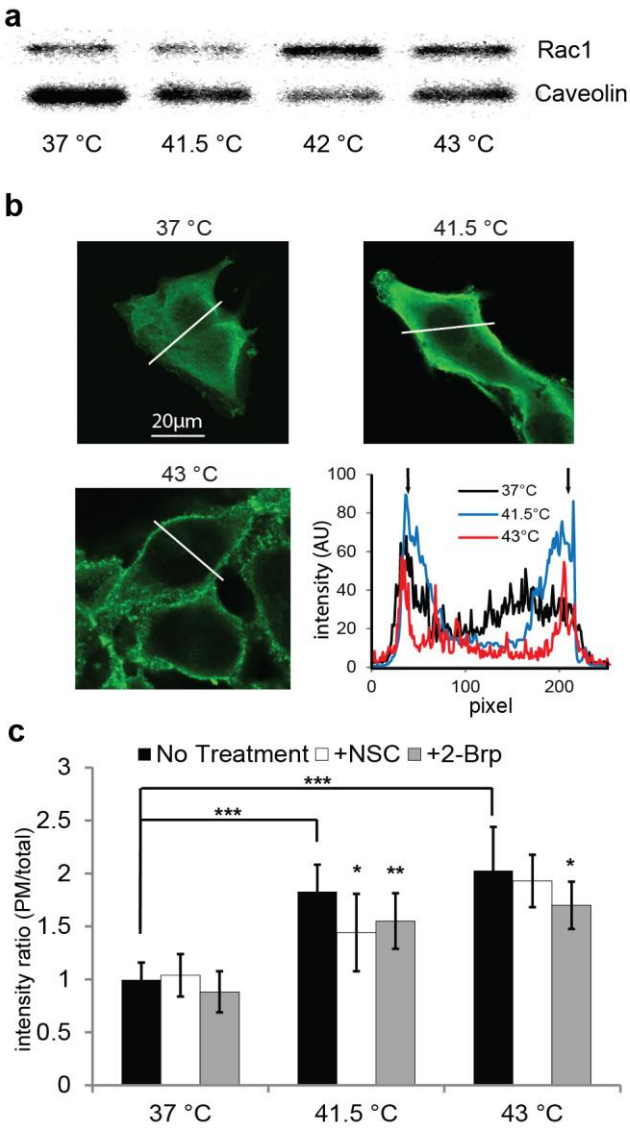
a
Rac1
Caveolin
37 °C
41.5 °C
42 °C
43 °C
b
37 °C
41.5 °C
20μm
43 °C
100
80
60
40
20
0
intensity (AU)
37°C
41.5°C
43°C
0
100
200
pixel
c
No Treatment
+NSC
+2-Brp
3
2.5
2
1.5
1
0.5
0
intensity ratio (PM/total)
***
***
*
**
*
37 °C
41.5 °C
43 °C

Fig.1

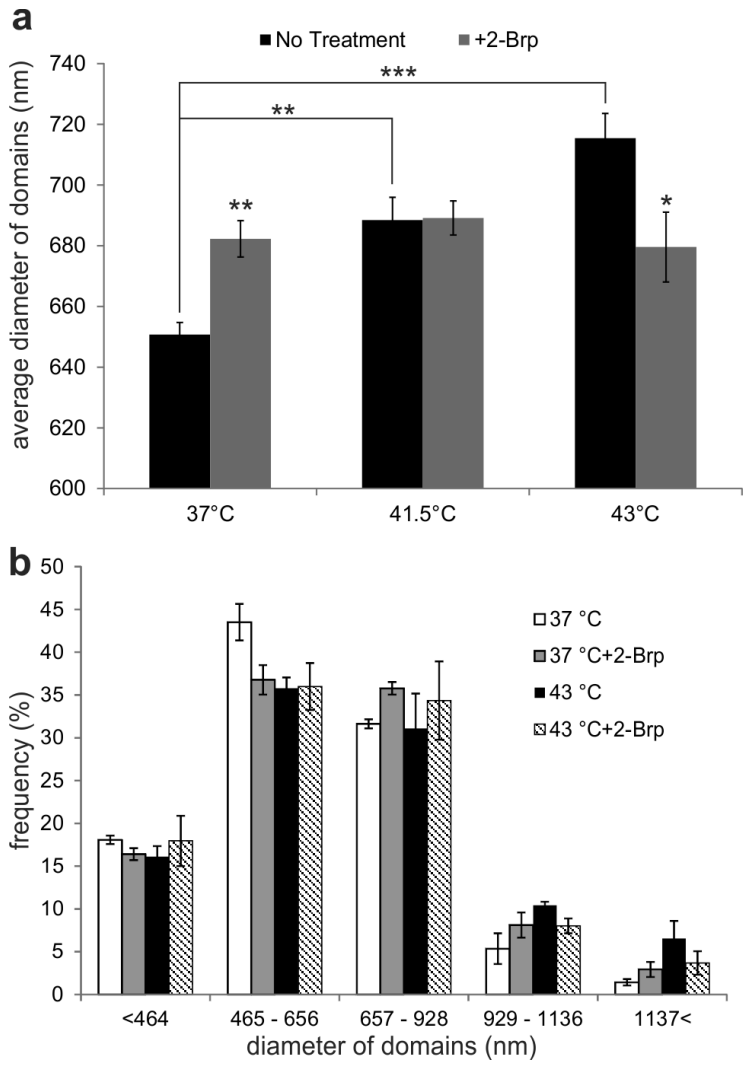
a
No Treatment
+2-Brp
average diameter of domains (nm)
740
720
700
680
660
640
620
600
***
**
**
*
37°C
41.5°C
43°C
b
frequency (%)
50
45
40
35
30
25
20
15
10
5
0
37 °C
37 °C+2-Brp
43 °C
43 °C+2-Brp
<464
465 - 656
657 - 928
929 - 1136
1137<
diameter of domains (nm)

Fig.2

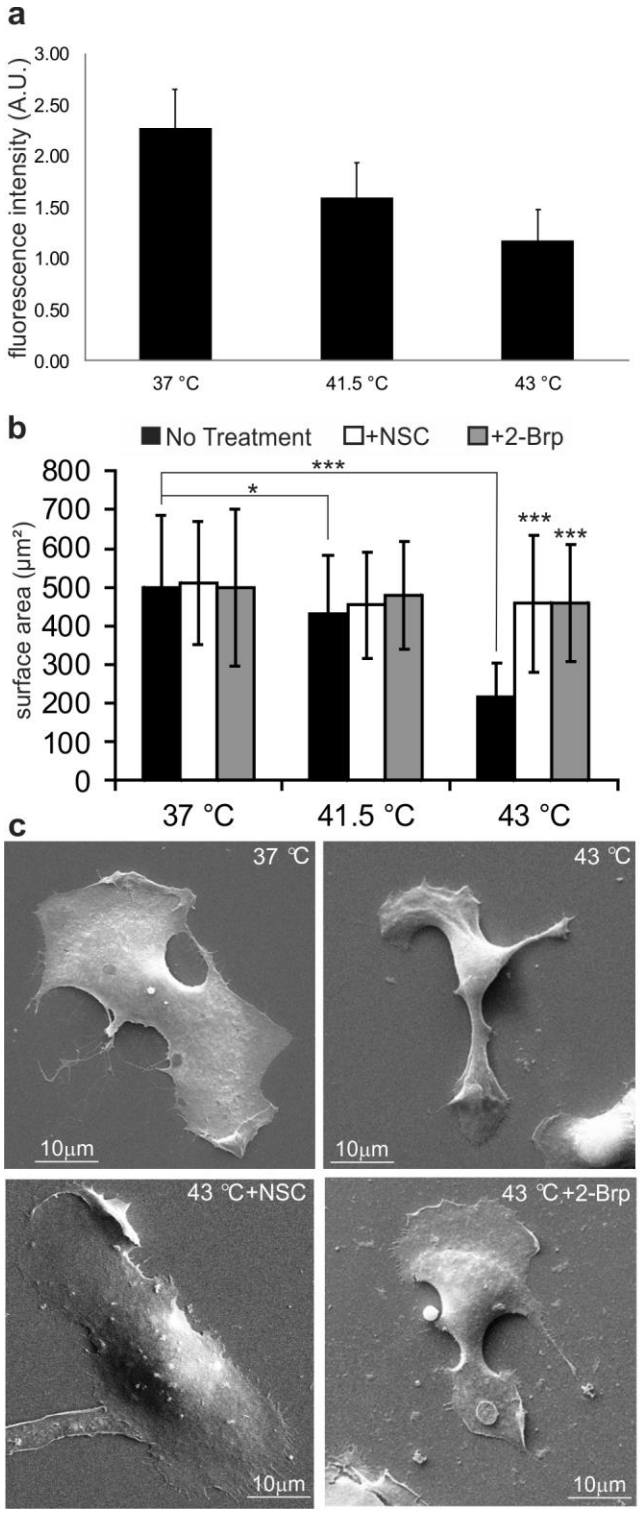
a
fluorescence intensity (A.U.)
3.00
2.50
2.00
1.50
1.00
0.50
0.00
37 °C
41.5 °C
43 °C
b
No Treatment
+NSC
+2-Brp
surface area (μm²)
800
700
600
500
400
300
200
100
0
*
***
***
***
37 °C
41.5 °C
43 °C
c
37 ℃
43 ℃
43 ℃+NSC
43 ℃+2-Brp
10μm
10μm
10μm
10μm

Fig.3

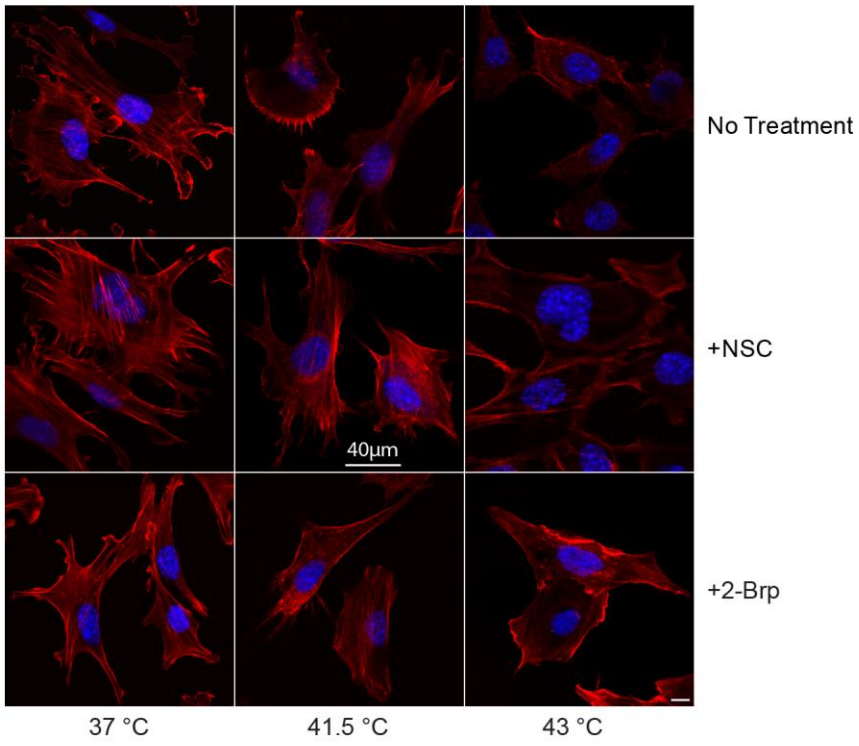

Fig.4

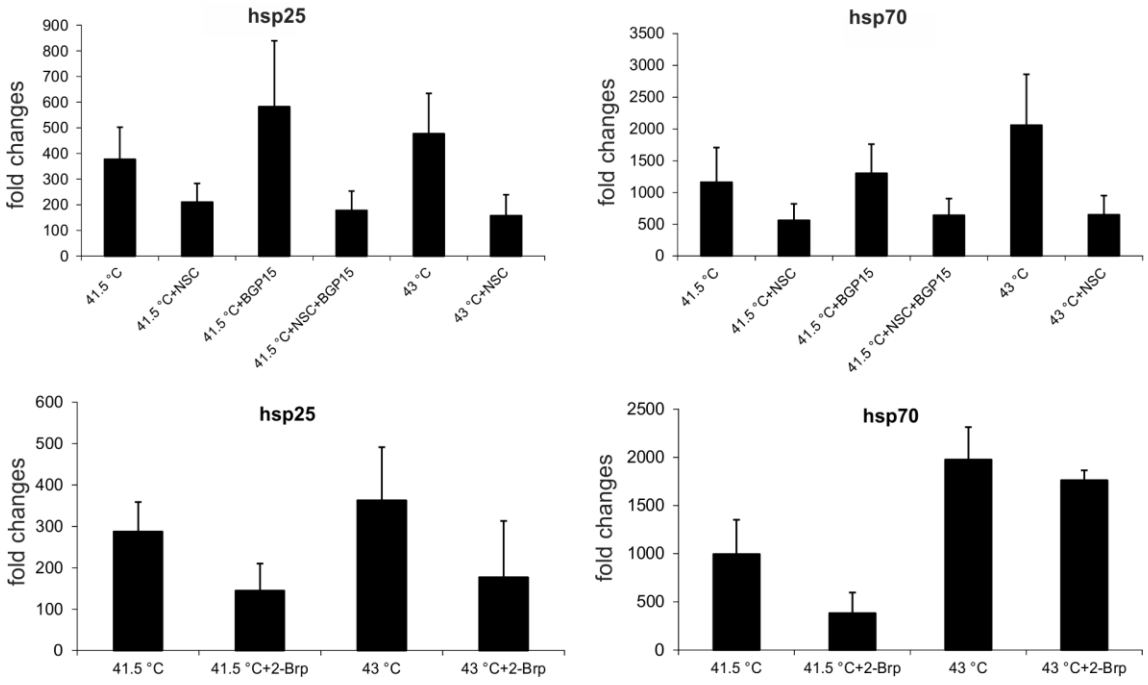
hsp25
fold changes
900
800
700
600
500
400
300
200
100
0
41.5 °C
41.5 °C+NSC
41.5 °C+BGP15
41.5 °C+NSC+BGP15
43 °C
43 °C+NSC
hsp70
fold changes
3500
3000
2500
2000
1500
1000
500
0
41.5 °C
41.5 °C+NSC
41.5 °C+BGP15
41.5 °C+NSC+BGP15
43 °C
43 °C+NSC
hsp25
fold changes
600
500
400
300
200
100
0
41.5 °C
41.5 °C+2-Brp
43 °C
43 °C+2-Brp
hsp70
fold changes
2500
2000
1500
1000
500
0
41.5 °C
41.5 °C+2-Brp
43 °C
43 °C+2-Brp

Fig.5

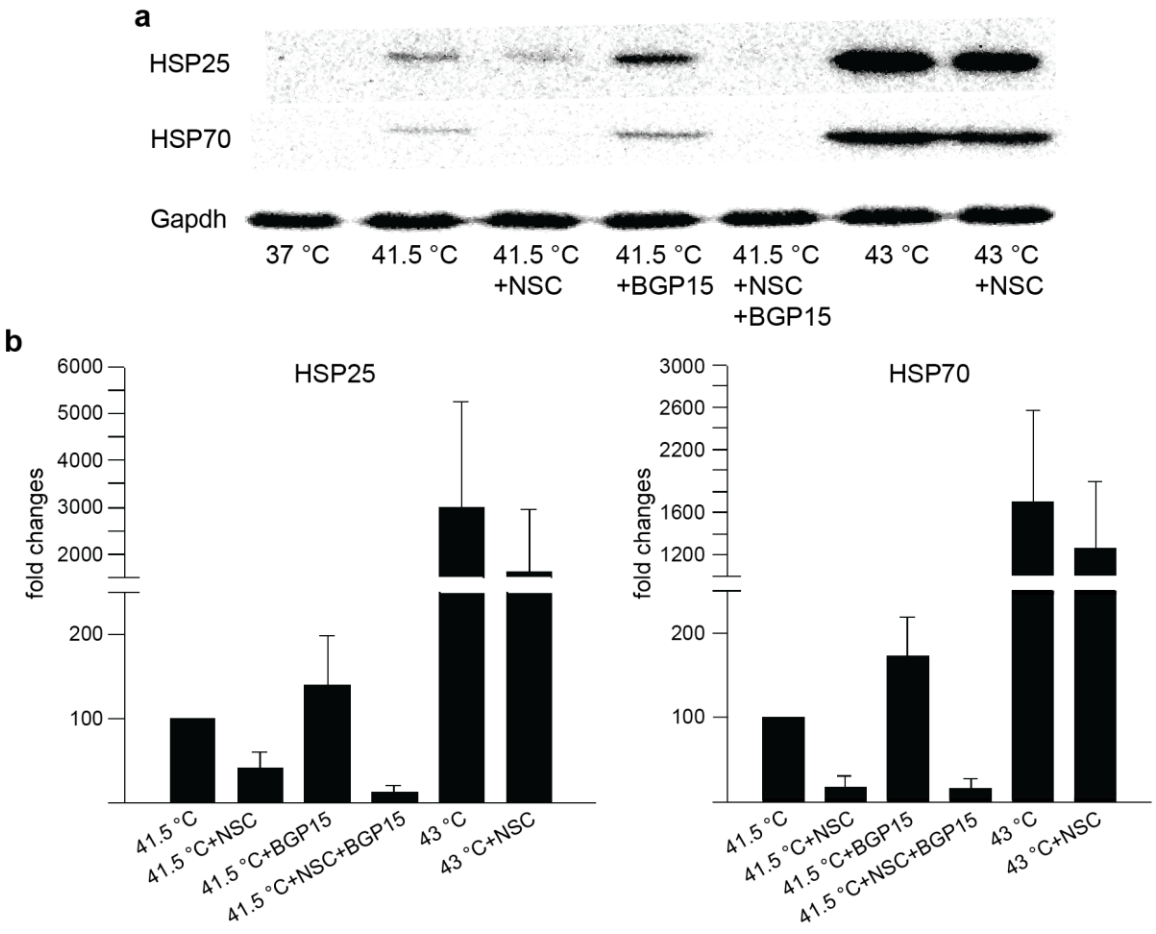
a
HSP25
HSP70
Gapdh
37 °C
41.5 °C
41.5 °C +NSC
41.5 °C +BGP15
41.5 °C +NSC +BGP15
43 °C
43 °C +NSC
b
HSP25
fold changes
6000
5000
4000
3000
2000
200
100
41.5 °C
41.5 °C+NSC
41.5 °C+BGP15
41.5 °C+NSC+BGP15
43 °C
43 °C+NSC
HSP70
fold changes
3000
2600
2200
1600
1200
200
100
41.5 °C
41.5 °C+NSC
41.5 °C+BGP15
41.5 °C+NSC+BGP15
43 °C
43 °C+NSC

Fig.6

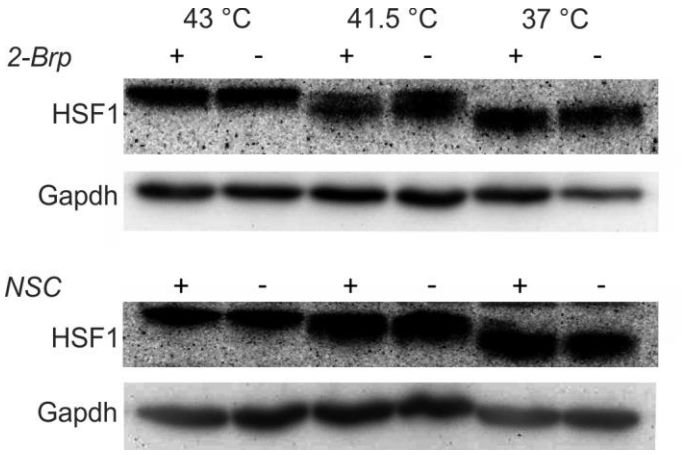

Fig.7